

# An Efficient Noise Removal Edge Detection Algorithm Based on Wavelet Transform

Ehsan Ehsaeyan\*

Department of Electrical and Computer engineering, Sirjan University of Technology, Sirjan, Iran  
ehsaeyan@sirjantech.ac.ir

Received: 18/Apr/2016

Revised: 15/Aug/2016

Accepted: 15/Sep/2016

## Abstract

In this paper, we propose an efficient noise robust edge detection technique based on odd Gaussian derivations in the wavelet transform domain. At first, new basis wavelet functions are introduced and the proposed algorithm is explained. The algorithm consists of two stage. The first idea comes from the response multiplication across the derivation and the second one is pruning algorithm which improves fake edges. Our method is applied to the binary and the natural grayscale image in the noise-free and the noisy condition with the different power density. The results are compared with the traditional wavelet edge detection method in the visual and the statistical data in the relevant tables. With the proper selection of the wavelet basis function, an admissible edge response to the significant inhibited noise without the smoothing technique is obtained, and some of the edge detection criteria are improved. The experimental visual and statistical results of studying images show that our method is feasibly strong and has good edge detection performances, in particular, in the high noise contaminated condition. Moreover, to have a better result and improve edge detection criteria, a pruning algorithm as a post processing stage is introduced and applied to the binary and grayscale images. The obtained results, verify that the proposed scheme can detect reasonable edge features and dilute the noise effect properly.

**Keywords:** Wavelet Transform; Edge Detection; Gaussian Filter; Multiscale Analysis; Noise Removal; Gaussian Bases; Wavelet Function Derivation; Admissibility Condition; Edge Criteria; N-connected Neighborhood.

## 1. Introduction

Nowadays, image processing has an important role in the proceeding of new science. Edge detection has various applications and is a useful tool in the registration, pattern recognition, topological recognition, image compression and other computer vision fields. Classical edge detectors like Roberts, Sobel and Prewitt have a simple structure which helps the time consumption saving. However, they have problems in the noisy condition and cannot discriminate the noise and background points properly. Furthermore, they cannot present images in automatic zoom and different scales.

One of the most popular algorithms is Gaussian-based edge detection due to the noise removal [1-2]. Canny proposed an edge detector based on Gaussian filter and identified three criteria for the optimal edge detector (good detection, good localization and low spurious response), which was successful in the noise free and high-contrast images [3]. Canny detector is a popular method which has been revised many times since it has been introduced [4-5]. But the noise interference is inevitable and natural images are almost polluted by the noise. The edge detection would be challenging and time consuming when the noise contaminates the image unexpectedly [6].

Another noise removal solution is the usage of scale-space theory. Multi-scale edge detection using wavelet transform has been introduced by Mallat [7]. Selecting a large scale can block the noise effect. In this condition,

spurious and false responses are weakened and disappear. But it occurs with the dislocation edge error too. On the other hand, selecting the low scale results in the noise sensitive detection. Therefore, there is a tradeoff between the good detection and the edge localization in noisy images. Multiresolution analysis has been introduced to obtain an intermediated compromised result. Zhang has continued Sadler [8] idea and proposed the scale multiplication to compromise between the localization error and the noise sensitive detection [9]. Zhu has used the scale multiplication technique based on the odd Gabor transform domain for the noise overcoming in the edge detection [10].

A number of Cellular Automata (CA)-based edge detectors have been developed recently due to the simplicity of the model and the potential for simultaneous removal of different types of noise in the process of detection [11-13].

With the increasing requirements of the accuracy of algorithms in the image edge detection, some intelligent algorithms are used, such as artificial neural network [14], fuzzy optimization [15], Genetic algorithm, ant colony optimization [16] and Particle Swarm Optimization.

Also, some new techniques have been developed in this field, which improve the edge detection performance, such as designing edge detector filters in potential field [17], Krawtchouk orthogonal polynomials [18], arctangent edge model [20], wavelet transform [19,21] and gravity field [22-23].

In this paper, we focus on the Gaussian edge detection and develop Canny edge detector by the derivation of

\* Corresponding Author

Gaussian wavelet function and improve results by introducing an algorithm which joints different edge maps. We show that this technique reduces spurious responses and improves edge detection criteria.

Our paper is organized as follows: Section 2 discusses the principal of the edge detection idea by the wavelet transform and introduces new wavelet functions based on  $n$ th derivative Gaussian, which are used in this paper for the edge detection. Section 3 deals with our scheme description and famous edge detection criteria and Section 4 demonstrates experimental results.

## 2. New Bases Introduction

Canny has used the first order derivative of the Gaussian filter as the wavelet function. We develop this idea to  $n$ th order derivative of the Gaussian filter. The wavelet functions derived from  $g(x, y)$  in the direction of  $x$  and  $y$  as:

$$\psi_x^n(x, y) = \frac{\partial^n g(x, y)}{\partial x^n} \quad (1a)$$

$$\psi_y^n(x, y) = \frac{\partial^n g(x, y)}{\partial y^n} \quad (1b)$$

$n = 1, 2, \dots$

These bases satisfy the admissibility condition and tend to 0 in  $\pm\infty$ . Assume  $g_s(x, y)$  be the smoothing function at the scale  $s$

$$g_s(x, y) = \frac{1}{2\pi s^2} e^{-\frac{1}{2s^2}(x^2+y^2)} \quad (2)$$

Hence, scaled wavelet bases are defined as

$$\psi_{s,x}^n(x, y) = s^n \frac{\partial^n g_s(x, y)}{\partial x^n} \quad (3a)$$

$$\psi_{s,y}^n(x, y) = s^n \frac{\partial^n g_s(x, y)}{\partial y^n} \quad (3b)$$

For an image  $f(x, y)$ , its wavelet transform has two elements in the  $x$  and  $y$  directions.

$$W_s^x(x, y) = f(x, y) * \psi_s^x(x, y) \quad (4-a)$$

$$W_s^y(x, y) = f(x, y) * \psi_s^y(x, y) \quad (4-b)$$

$$M_s f(x, y) = \sqrt{W_s^x(x, y)^2 + W_s^y(x, y)^2} \quad (4-c)$$

The points at which their modulus values ( $M_s f(x, y)$ ) are the local maximums correspond to abrupt change points in the corresponding positions of the smooth image or the position of the sharp and steep changes, whose sizes reflect the gray strengths in the positions. So, as long as we detect the local maximum value points of the wavelet transform series modulus along the gradient direction, the edge points of the image are gained.

## 3. Method Description and Analysis Parameters

In this section, we describe the proposed method. Then some famous criteria are discussed briefly, which are used in experimental results.

### 3.1 Method Description

Traditionally, first derivation of the Gaussian wavelet is considered as an edge detector [3]. Finding local maxima of absolute  $M(x, y)$  in  $A(x, y)$  direction yields edge points (magnitude and orientation). Another method is the usage of the second derivation of the Gaussian filter response and finding zero-crossing points, which is very sensitive to the noise. Zhang improved results by the scale multiplication method [9]. We complete Zhang method and introduce here a novel technique of the Gaussian wavelet edge detection to refine the noise interference. This technique is based on the multiplication of  $\psi_s^n(x, y)$  edge responses not only across the scale  $s$ , but across the derivation  $n$ . This procedure has two freedom degree parameters to adjust noise and the edge dislocation. Fig 1 shows the block diagram of the proposed method. Our method consists of five steps:

- 1- Input noisy image which has been corrupted by AWGN.
- 2- Calculate  $\psi_{s,x}^n(x, y)$  and  $\psi_{s,y}^n(x, y)$  according to Eq (3) in unit *scale* and  $n = 1, 2, 3$ . The length of filters is 7.
- 3- Obtain relevant coefficients in  $x$  and  $y$  directions by convolution of calculated bases in step 2 with the noisy image.
- 4- Prepare the edge maps of every derivation (i.e.  $n=1, 3, 5$ ) according to Eq (4-c) which named  $W_s^n(x, y)$ . These results are shown in the first stage of Figure 1.
- 5- Apply pruning algorithm to different edge maps and yield a result with higher quality and lower fake edges.

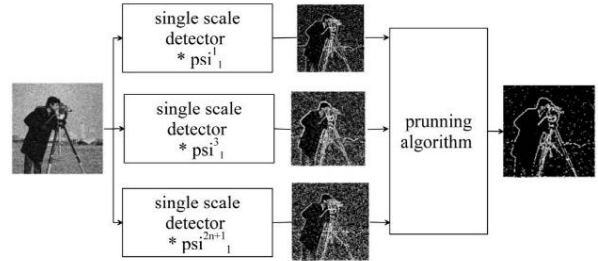


Fig. 1. Block diagram of proposed method

### 3.2 Analysis Criteria

Pratt [25] introduced a criterion that shows the quantity performance of edge detection, which is used in much research [10, 24]. This parameter is called *figure of merit* and defined as:

$$F = \frac{1}{\max\{N_I, N_A\}} \sum_{i=1}^{N_A} \frac{1}{1 + \alpha d^2(i)} \quad (5)$$

Where  $N_I$  is the number of true edges, and  $N_A$  represents the number of marked edges by the detector algorithm.  $\alpha$  is a penalty scaling number that controls false edges and is set on 1/9 in this paper like Pratt work.  $d$  means the Euclidian distance between the point detected by the algorithm procedure and marked as the edge point and its actual edge in the reference map. There

are three types of distance definition between two pixels  $(x_1, y_1)$  and  $(x_2, y_2)$  which are used in this paper as follows:

- Cityblock: in 2D space, the cityblock distance is defined as  $|x_1-x_2|+|y_1-y_2|$
- Chessboard: which is identified by  $\max(|x_1-x_2|,|y_1-y_2|)$
- Quasi-Euclidean: the quasi-Euclidean distance is calculated by:

$$d_{quasi-euclidean} = \begin{cases} |x_1 - x_2| + (\sqrt{2} - 1)|y_1 - y_2| & |x_1 - x_2| > |y_1 - y_2| \\ (\sqrt{2} - 1)|x_1 - x_2| + |y_1 - y_2| & otherwise \end{cases} \quad (6)$$

Second parameter is based on the distance between marked edges and true edges. Root mean square localization error is denoted by  $D$  and designed by Zhang [9]:

$$D = \sqrt{\frac{1}{N} \sum_{i=1}^N (p_g(i) - p_d(i))^2} \quad (7)$$

where  $N$  in this formula is the number of edge points. The actual edge position is denoted by  $p_g$  and the detected edge point by the algorithm is denoted by  $p_d$ .

The edges are classified in four groups in the edge detection process:

*True positive (TP)*: these edges are actual edges, and we detected them correctly. An edge detector would be more powerful that has a higher TP edges result.

*False positive (FP)*: this criterion refers to the amount of the edges that are not real edges; but we detected them as true edges.

*True negative (TN)*: these points are not edges and we ignored them correctly. TP has a reverse relationship with FP in most cases. The greater true negative means the better edge detection result.

*False negative (FN)*: we neglected this type of points as edges. But they are true edges. Lower FP means better edge quality.

*True positive rate (TPR)*: this normalized criterion contains correct and false detection pixels, and shows the sensitivity of results. True positive rate is calculated as:

$$TPR = \frac{TP}{TP + FN} \quad (8)$$

*False positive rate (FPR)*: conversely, FPR refers to the error of edge detecting. False positive rate is between 0 to 1 and specified by:

$$FPR = \frac{FP}{FP + TN} \quad (9)$$

*Precision (PREC)*: another evaluation parameter declares how the percentage of marked edge points is true. Precision is obtained from [2]:

$$PREC = \frac{TP}{TP + FP} \quad (10)$$

*F alpha-measure (Fa)*: F alpha-measure shows the overall quality and is given by [26]:

$$F_\alpha = \frac{PREC \cdot TPR}{\alpha PREC + (1 - \alpha) TPR} \quad (11)$$

Where  $\alpha$  is a scaling constant between 0 and 1.

*Accuracy*: it shows the precision of diagnostic true edges in edge detection. Accuracy is delivered by percentage and obtained from:

$$accuracy (\%) = 100 \times \frac{TP + TN}{TP + TN + FP + FN} \quad (12)$$

## 4. Experimental Results

In this section, the ability of proposed edge detector is shown. We present results in visual and statistical modes.

### 4.1 Visual Results

In this part, the wavelet response of proposed bases is investigated. We applied three wavelet bases  $\psi^1(x, y)$ ,  $\psi^3(x, y)$  and  $\psi^5(x, y)$  to the images. The results are illustrated in Fig 2. Two types of image were considered in this paper: binary ('WAVELET TRANSFORM') and grayscale ('Lena' and 'cameraman') with the size of 256\*256 pixels.

Each image has two columns. First one is a noise free image and its  $W_1^1(x, y)$ ,  $W_1^3(x, y)$  and  $W_1^5(x, y)$  wavelet edges respectively. And second column shows the image with an exploited edge from the wavelet coefficient at scale  $s = 1$ . These results are achieved after applying the threshold to wavelet coefficients at the scale  $s=1$ . The images are corrupted by additive white Gaussian noise with the different variance. We find out, there is a little difference between  $W_s^1(x, y)$ ,  $W_s^3(x, y)$  and  $W_s^5(x, y)$ . So all of them can be used in edge detection separately. In much research, first order derivative of the smooth function is used as the edge detector.

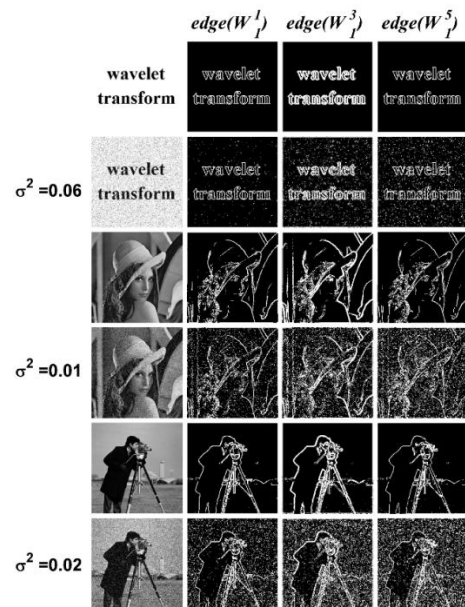


Fig. 2. First, third and fifth Gaussian derivation wavelet response with different noise power density in scale  $s=1$ . First columns of images are noise free.

Fig 3 shows the results of the edge detection based on first, third and fifth order derivation of the Gaussian smooth function (response of  $\psi^1(x, y)$ ,  $\psi^3(x, y)$  and  $\psi^5(x, y)$ ) in ideal (first rows) and various noise power (second and third rows) cases. The first rows indicate the noise free response where coefficients multiplication,  $W_s^1(x, y) \times W_s^3(x, y)$  or  $W_s^1(x, y) \times W_s^3(x, y) \times W_s^5(x, y)$  extenuates thick edges. When the image is polluted a little by noise, the best choice is the use of single  $W_s^i(x, y)$  for the edge detection. When the noise power density is considerable, and we cannot ignore the effect of noise, it is better to use  $W_s^1(x, y) \times W_s^3(x, y)$  instead of the traditional one for edge detection. Assume that the image is contaminated by noise significantly. The best choice is  $W_s^1(x, y) \times W_s^3(x, y) \times W_s^5(x, y)$  where the wrong edges number is lowest and true edges remain meaningful.

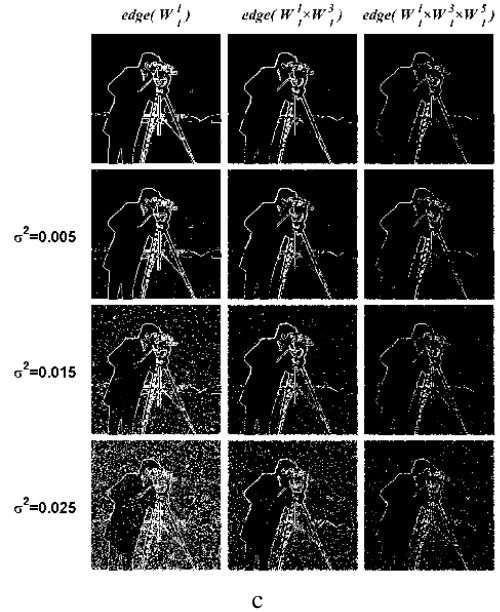
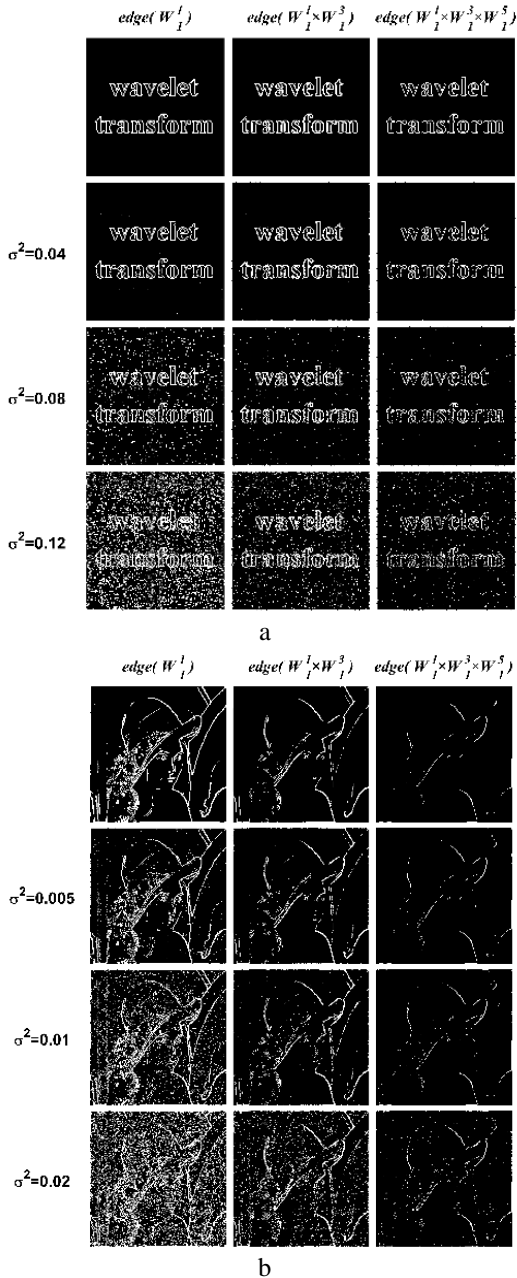


Fig. 3. Multiplication of wavelet coefficients according to Gaussian bases in different noise condition

### 4.2 Statistical Results

The previous part shows the edge detection in the visual scene. In this part, the statistical results of the parameters which have been introduced in section 2, are calculated and presented in tables for the discussion and comparison. We can investigate the edge responses and obtain results similar to the ones in the previous part. Table 1 shows the calculated statistical parameters of the three images ('wavelet transform', 'Lena', 'cameraman') with the different noise power.

Table 1. Statistical results of edge detection.  $d1$ ='cityblock',  $d2$ ='chessboard' and  $d3$ ='quasi-Euclidian' distance definition (refer to section 3)

		'wavelet transform' binary image			
		$\sigma^2 = 0.04$	$\sigma^2 = 0.08$	$\sigma^2 = 0.12$	
$W_1^1$ (traditional wavelet edge detection)	F	d1	0.9295	0.6522	0.4367
		d2	0.9303	0.6601	0.4489
		d3	0.9299	0.6556	0.4418
	D	d1	0.2495	0.8323	1.3432
		d2	0.2330	0.8542	1.3686
		d3	0.2367	0.8183	1.3130
	TPR		0.9168	0.9143	0.9141
	FPR		0.0032	0.0546	0.1821
	PREC		0.9576	0.5655	0.2806
	$F_a$		0.9367	0.6988	0.4294
ACCURACY		99.1074	94.3176	82.4844	
$W_1^1 \times W_1^3$ (proposed in this paper)	F	d1	0.9284	0.8157	0.6417
		d2	0.9306	0.8201	0.6500
		d3	0.9293	0.8175	0.6453
	D	d1	0.3926	0.6173	0.9527
		d2	0.4099	0.6499	0.9683
		d3	0.3835	0.6099	0.9303
	TPR		0.8993	0.8506	0.8129
	FPR		0.0101	0.0266	0.0670
	PREC		0.8737	0.7127	0.4852
	$F_a$		0.8863	0.7756	0.6077
ACCURACY		98.3368	96.4508	92.4316	
$W_1^1 \times W_1^3 \times W_1^5$ (proposed in this paper)	F	d1	0.7685	0.7238	0.7324
		d2	0.7687	0.7249	0.7371
		d3	0.7686	0.7242	0.7344
	D	d1	0.1242	0.3149	0.6543
		d2	0.1285	0.3520	0.6702
		d3	0.1190	0.3268	0.6458
	TPR		0.7642	0.6988	0.6472
	FPR		7.7289e-04	0.0061	0.0232
	PREC		0.9872	0.8992	0.6843
	$F_a$		0.8615	0.7865	0.6652
ACCURACY		98.2285	97.2641	95.3033	

$d1$ ='cityblock'  $d2$ ='chessboard'  $d3$ ='quasi-Euclidean'

Table 1. Continue

		lena			
		$\sigma^2 = 0.005$	$\sigma^2 = 0.01$	$\sigma^2 = 0.02$	
$W_1^1$ (traditional wavelet edge detection)	F	d1	0.8432	0.7083	0.5671
		d2	0.8563	0.7378	0.6096
		d3	0.8486	0.7203	0.5847
	D	d1	0.6980	1.2090	1.6069
		d2	0.7536	1.2742	1.6667
		d3	0.6575	1.1517	1.5292
	TPR		0.7804	0.7877	0.7663
	FPR		0.0222	0.0880	0.2224
	PREC		0.8183	0.5342	0.3062
	$F_\alpha$		0.7989	0.6367	0.4376
	ACCURACY		<b>95.5383</b>	89.7903	77.6306
$W_1^1 \times W_1^1$ (proposed in this paper)	F	d1	0.3829	0.4289	0.6989
		d2	0.3847	0.4329	0.7293
		d3	0.3836	0.4305	0.7114
	D	d1	0.3558	0.5734	1.2330
		d2	0.3902	0.6179	1.3280
		d3	0.3449	0.5449	1.1702
	TPR		0.3738	0.3992	0.5003
	FPR		0.0028	0.0086	0.0664
	PREC		0.9450	0.8564	0.4913
	$F_\alpha$		0.5357	0.5446	0.4957
	ACCURACY		92.6422	<b>92.4179</b>	88.4430
$W_1^1 \times W_1^3 \times W_1^5$ (proposed in this paper)	F	d1	0.0930	0.1190	0.2251
		d2	0.0930	0.1191	0.2284
		d3	0.0930	0.1191	0.2265
	D	d1	0	0.2042	0.7327
		d2	0	0.1957	0.7575
		d3	0	0.1667	0.6865
	TPR		0.0930	0.1182	0.2012
	FPR		1.7213e-05	1.8935e-04	0.0071
	PREC		0.9986	0.9877	0.7846
	$F_\alpha$		0.1701	0.2112	0.3202
	ACCURACY		89.6988	89.9704	<b>90.3015</b>

d1='cityblock' d2='chessboard' d3='quasi-Fuclidean'

Table 1. Continue

		cameraman			
		$\sigma^2 = 0.005$	$\sigma^2 = 0.015$	$\sigma^2 = 0.025$	
$W_1^1$ (traditional wavelet edge detection)	F	d1	0.8955	0.7175	0.4991
		d2	0.8972	0.7298	0.5216
		d3	0.8961	0.7221	0.5074
	D	d1	0.2807	0.9335	1.4477
		d2	0.3041	0.9681	1.5200
		d3	0.2631	0.9012	1.4111
	TPR		0.8803	0.8378	0.8565
	FPR		0.0061	0.0526	0.1879
	PREC		0.9363	0.6170	0.3157
	$F_\alpha$		0.9074	0.7107	0.4614
	ACCURACY		<b>98.3490</b>	93.7302	81.6223
$W_1^1 \times W_1^3$ (proposed in this paper)	F	d1	0.6944	0.7255	0.6653
		d2	0.6967	0.7316	0.6809
		d3	0.6953	0.7278	0.6710
	D	d1	0.3453	0.5952	1.0569
		d2	0.3935	0.6434	1.1130
		d3	0.3389	0.5902	1.0267
	TPR		0.6724	0.6474	0.6605
	FPR		0.0056	0.0199	0.0662
	PREC		0.9242	0.7668	0.5024
	$F_\alpha$		0.7785	0.7020	0.5707
	ACCURACY		96.4828	<b>94.9493</b>	90.8676
$W_1^1 \times W_1^3 \times W_1^5$ (proposed in this paper)	F	d1	0.4128	0.4109	0.4783
		d2	0.4128	0.4115	0.4827
		d3	0.4128	0.4111	0.4800
	D	d1	0.0201	0.2745	0.7557
		d2	0.0201	0.2933	0.7950
		d3	0.0201	0.2671	0.7351
	TPR		0.4126	0.4026	0.4272
	FPR		1.0082e-04	0.0023	0.0155
	PREC		0.9976	0.9469	0.7358
	$F_\alpha$		0.5837	0.5650	0.5405
	ACCURACY		94.5923	94.3024	<b>93.3258</b>

d1='cityblock' d2='chessboard' d3='quasi-Fuclidean'

## 5. Improved Algorithm

In the previous section, we saw that  $W_s^1(x, y)$  (traditional wavelet edge detection) was useful in low noise condition and had good results in parameters listed in Table 1. But its drawback is the acting on the medium and high noise level. In other words, it is very sensitive to noise

contaminating. In this condition,  $W_s^1(x, y) \times W_s^3(x, y)$  or  $W_s^1(x, y) \times W_s^3(x, y) \times W_s^5(x, y)$  is introduced as a method to refine noise.  $W_s^1(x, y) \times W_s^3(x, y)$  and  $W_s^1(x, y) \times W_s^3(x, y) \times W_s^5(x, y)$  are powerful to remove spurious responses where created by the noise. Their suppressing noise parameters such as D, FPR, PREC,  $F_\alpha$  and Accuracy have been better than  $W_s^1(x, y)$  parameters.

But the edge quality was low, and it could detect only main and thick edges and had low TPR and Figure of merit criteria.  $W_s^1(x, y) \times W_s^3(x, y)$  or  $W_s^1(x, y) \times W_s^3(x, y) \times W_s^5(x, y)$  kills noise and details simultaneously. So in high polluted images another algorithm is essential to pick up good characteristics of  $W_s^1(x, y)$  such as TPR and F and pick up good characteristics of  $W_s^1(x, y) \times W_s^3(x, y) \times W_s^5(x, y)$  such as FPR and PREC to improve the edge detection criteria and handles a reasonable response. This algorithm must be applied as a post-processing to result edges, i.e. wavelet coefficients after a thresholding process. An improved edge detection algorithm named pruning algorithm is introduced here. Pruning algorithm is a post-processing stage that applied to binary image (detected edge map). It is useful where there are similar edge maps such as multiresolution levels of an image, and we want to fuse them. In pruning algorithm, a binary frame with the complete edge and also with the high polluted noise is chosen as the initial edge image. Other frames are used to improve edges in the initial edge image.

This algorithm uses  $W_s^1(x, y)$  as a basic edge frame. In this process, all the detected points in  $W_s^1(x, y)$  are considered as candidate edges and tries to remove false edges by searching the neighborhood of pixels in other frames like  $W_s^1(x, y) \times W_s^3(x, y)$  or  $W_s^1(x, y) \times W_s^3(x, y) \times W_s^5(x, y)$ .

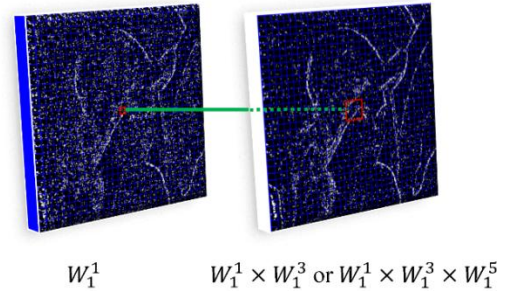


Fig. 4. N-connected neighborhood for searching areas

The pruning algorithm is as follows:

1- Define an n-connected neighborhood for searching areas as shown in Fig 4.

2- For each pixel belonging to  $W_s^1(x, y)$ , determine this pixel and study n-connected neighborhood in  $W_s^1(x, y) \times W_s^3(x, y)$  or  $W_s^1(x, y) \times W_s^3(x, y) \times W_s^5(x, y)$ . If FPR is more important to us,  $W_s^1(x, y) \times W_s^3(x, y) \times W_s^5(x, y)$  is selected for searching area and if accuracy and TPR are more important in the edge detection,  $W_s^1(x, y) \times W_s^3(x, y)$  is a better choice.

3- To achieve noise reduction, if the number of detected edges in  $W_s^1(x, y) \times W_s^3(x, y)$  or  $W_s^1(x, y) \times$

$W_s^3(x, y) \times W_s^5(x, y)$  is more than  $N$ ,  $p(i, j)$  is denoted as a real pixel, otherwise  $p(i, j)$  in  $W_s^1(x, y)$  changes to zero.

This algorithm applied to study images and results are shown in Fig 5 and Table 2.

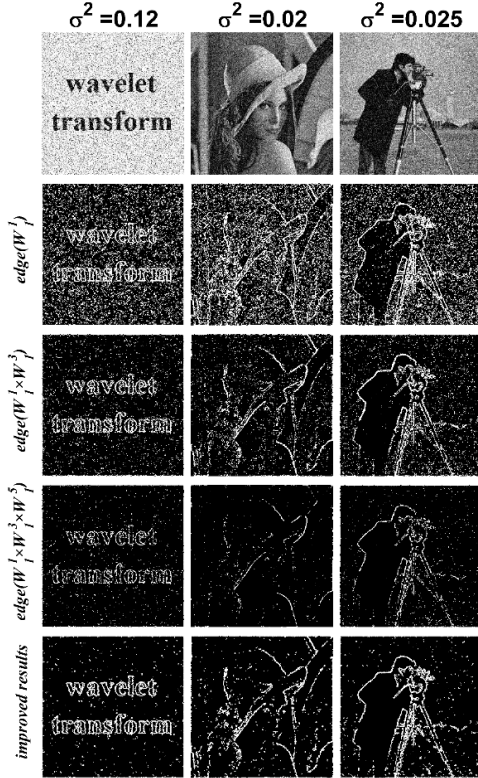


Fig. 5. Applied pruning algorithm to noisy images

The results of the proposed algorithm have a less edge loss and higher noise blocking. According to Table 2, most of the statistical parameters like TPR are compensated after applying the pruning algorithm. Meanwhile, the improved results have the greatest  $F$ ,  $F_\alpha$  and Accuracy.

This procedure would be mixed with the scale edge i.e. the scaled edge frames with  $s=1,2,\dots$  are chosen for the searching area procedure. In this condition due to refining noise in the higher scale, the rate of false edge detection reduced significantly. Also by selecting a lower scale as the initial edge frame, true location is preserved. However, a computational cost is exposed to the edge detection.

Table. 2. Statistical results of the applied pruning algorithm

		F			D		
		d1	d2	d3	d1	d2	d3
'wavelet transform' image	$W_1^1$	0.437	0.449	0.442	1.343	1.369	1.313
	$W_1^1 \times W_1^3$	0.642	0.65	0.645	0.953	0.968	0.93
	$W_1^1 \times W_1^3 \times W_1^5$	0.732	0.737	0.734	0.654	0.67	0.646
	Improved	0.7627	0.7691	0.7655	0.7475	0.7575	0.7252
lenna	$W_1^1$	0.5671	0.6096	0.5847	1.6069	1.6667	1.5292
	$W_1^1 \times W_1^3$	0.6989	0.7293	0.7114	1.233	1.328	1.1702
	$W_1^1 \times W_1^3 \times W_1^5$	0.2251	0.2284	0.2265	0.7327	0.7575	0.6865
	Improved	0.7043	0.7231	0.7119	0.9906	1.0555	0.9472
cameram an	$W_1^1$	0.499	0.522	0.507	1.448	1.52	1.411
	$W_1^1 \times W_1^3$	0.665	0.681	0.671	1.057	1.113	1.027
	$W_1^1 \times W_1^3 \times W_1^5$	0.478	0.483	0.48	0.756	0.795	0.735
	Improved	0.8106	0.8203	0.8144	0.7839	0.8272	0.7553

Table. 2. Continue

		TPR	FPR	PREC	$F_\alpha$	ACCURACY
'wavelet transform' image	$W_1^1$	0.914	0.182	0.281	0.429	82.4844
	$W_1^1 \times W_1^3$	0.813	0.067	0.485	0.608	92.4316
	$W_1^1 \times W_1^3 \times W_1^5$	0.647	0.023	0.684	0.665	95.3033
	Improved	0.904	0.035	0.665	0.767	<b>96.0297</b>
lenna	$W_1^1$	0.7663	0.2224	0.3062	0.4376	77.6306
	$W_1^1 \times W_1^3$	0.5003	0.0664	0.4913	0.4957	88.443
	$W_1^1 \times W_1^3 \times W_1^5$	0.2012	0.0071	0.7846	0.3202	90.3015
	Improved	0.5657	0.041	0.6387	0.6	<b>91.4337</b>
cameram an	$W_1^1$	0.857	0.188	0.316	0.461	81.6223
	$W_1^1 \times W_1^3$	0.661	0.066	0.502	0.571	90.8676
	$W_1^1 \times W_1^3 \times W_1^5$	0.427	0.016	0.736	0.541	93.3258
	Improved	0.7523	0.0317	0.706	0.7284	<b>94.8441</b>

## 6. Conclusions

An efficiency edge detection algorithm to remove spurious noise based on nth order derivative of Gaussian wavelet is presented in this paper. To approach the goal, first a new set of wavelet bases is introduced. After that, a new algorithm based on the wavelet coefficients multiplication is presented. We showed that how the use of higher order of Gaussian derivations can improve edge detection criteria. Our algorithm is applied to noisy binary and grayscale images in order to verify the efficiency of the proposed scheme for these two types of images and the results are carried out in both visual and statistical data. The results are compared with the traditional wavelet transform edge detection and investigated edge detection parameters. Our method has two freedom parameters (nth order derivative and the scale) to compare the basic Gaussian wavelet edge detection, which has a single parameter (scale) to adjust the resolution and noise refining. Finally, a neighborhood searching algorithm as a post processing stage is applied to improve the proposed method. The experimental results verified that our scheme is capable of improving image criteria on demand.

## References

- [1] F. Guo, Y. Yang, B. Chen, and L. Guo, "A novel multi-scale edge detection technique based on wavelet analysis with application in multiphase flows," *Powder Technology*, vol. 202, no. 1-3, pp. 171–177, Aug. 2010.
- [2] C. Lopez-Molina, B. De Baets, H. Bustince, J. Sanz, and E. Barrenechea, "Multiscale edge detection based on Gaussian smoothing and edge tracking," *Knowledge-Based Systems*, vol. 44, pp. 101–111, May 2013.
- [3] J. Canny, "A computational approach to edge detection," *IEEE Transactions on Pattern Analysis and Machine Intelligence*, vol. PAMI-8, no. 6, pp. 679–698, Nov. 1986.
- [4] W. McIlhagga, "The canny edge detector revisited," *International Journal of Computer Vision*, vol. 91, no. 3, pp. 251–261, Oct. 2010.
- [5] L. Ding and A. Goshtasby, "On the canny edge detector," *Pattern Recognition*, vol. 34, no. 3, pp. 721–725, Mar. 2001.
- [6] R. C. Gonzalez, R. E. Woods, D. J. Czitrom, and S. Armitage, *Digital image processing*, 3rd ed. United States: Prentice Hall, 2007.
- [7] S. Mallat and S. Zhong, "Characterization of signals from multiscale edges," *IEEE Transactions on Pattern Analysis and Machine Intelligence*, vol. 14, no. 7, pp. 710–732, Jul. 1992.
- [8] B. M. Sadler and A. Swami, "Analysis of multiscale products for step detection and estimation," *IEEE Transactions on Information Theory*, vol. 45, no. 3, pp. 1043–1051, Apr. 1999. [9] L. Zhang and P. Bao, "Edge detection by scale multiplication in wavelet domain," *Pattern Recognition Letters*, vol. 23, no. 14, pp. 1771–1784, Dec. 2002.
- [9] Z. Zhu, H. Lu, and Y. Zhao, "Scale multiplication in odd Gabor transform domain for edge detection," *Journal of Visual Communication and Image Representation*, vol. 18, no. 1, pp. 68–80, Feb. 2007.
- [10] M. Hasanzadeh Mofrad, S. Sadeghi, A. Rezvanian, and M. R. Meybodi, "Cellular edge detection: Combining cellular automata and cellular learning automata," *AEU - International Journal of Electronics and Communications*, vol. 69, no. 9, pp. 1282–1290, Sep. 2015.
- [11] S. Uguz, U. Sahin, and F. Sahin, "Edge detection with fuzzy cellular automata transition function optimized by PSO," *Computers & Electrical Engineering*, vol. 43, pp. 180–192, Apr. 2015.
- [12] S. Amrogowicz and Y. Zhao, "An edge detection method using outer totalistic cellular Automata," *Neurocomputing*, Jun. 2016.
- [13] J. Gu, Y. Pan, and H. Wang, "Research on the improvement of image edge detection algorithm based on artificial neural network," *Optik - International Journal for Light and Electron Optics*, vol. 126, no. 21, pp. 2974–2978, Nov. 2015.
- [14] C. I. Gonzalez, P. Melin, J. R. Castro, O. Castillo, and O. Mendoza, "Optimization of interval type-2 fuzzy systems for image edge detection," *Applied Soft Computing*, vol. 47, pp. 631–643, Oct. 2016.
- [15] X. Liu and S. Fang, "A convenient and robust edge detection method based on ant colony optimization," *Optics Communications*, vol. 353, pp. 147–157, Oct. 2015.
- [16] G. Ma, C. Liu, and D. Huang, "The removal of additional edges in the edge detection of potential field data," *Journal of Applied Geophysics*, vol. 114, pp. 168–173, Mar. 2015.
- [17] D. Rivero-Castillo, H. Pijeira, and P. Assunção, "Edge detection based on Krawtchouk polynomials," *Journal of Computational and Applied Mathematics*, vol. 284, pp. 244–250, Aug. 2015.
- [18] N. Decoster, S. G. Roux, and A. Arnéodo, "A wavelet-based method for multifractal image analysis. II. Applications to synthetic multifractal rough surfaces," *The European Physical Journal B*, vol. 15, no. 4, pp. 739–764, Jun. 2000.
- [19] Q. Sun, Y. Hou, and Q. Tan, "A subpixel edge detection method based on an arctangent edge model," *Optik - International Journal for Light and Electron Optics*, vol. 127, no. 14, pp. 5702–5710, Jul. 2016.
- [20] G. J. Tu and H. Karstoft, "Logarithmic dyadic wavelet transform with its applications in edge detection and reconstruction," *Applied Soft Computing*, vol. 26, pp. 193–201, Jan. 2015.
- [21] B. Zuo and X. Hu, "Edge detection of gravity field using eigenvalue analysis of gravity gradient tensor," *Journal of Applied Geophysics*, vol. 114, pp. 263–270, Mar. 2015.
- [22] J. Wang, X. Meng, and F. Li, "Improved curvature gravity gradient tensor with principal component analysis and its application in edge detection of gravity data," *Journal of Applied Geophysics*, vol. 118, pp. 106–114, Jul. 2015.
- [23] M.-Y. Shih and D.-C. Tseng, "A wavelet-based multiresolution edge detection and tracking," *Image and Vision Computing*, vol. 23, no. 4, pp. 441–451, Apr. 2005.
- [24] Pratt, W.K.: 'Digital Image Processing', (John Wiley & Sons, New York, USA, 2001. Eased)
- [25] M. K. Geetha and S. Palanivel, "Video classification and shot detection for video retrieval applications," *International Journal of Computational Intelligence Systems*, vol. 2, no. 1, pp. 39–50, 2009.

**Ehsan Ehsaeyan** received the B.Sc degree in electrical engineering from Shahed University, Tehran, Iran in 2005. He received the M.Sc degree in communication engineering from Shahid Bahonar University, Kerman, Iran, in 2009. His area research interests include Image Processing and Digital Signal Processing.